

Improving photoresponsivity in GaAs film grown on Al-induced-crystallized Ge on an insulator

Cite as: AIP Advances **10**, 015153 (2020); <https://doi.org/10.1063/1.5138677>

Submitted: 15 November 2019 . Accepted: 08 January 2020 . Published Online: 28 January 2020

T. Nishida, T. Suemasu , and K. Toko

COLLECTIONS

Paper published as part of the special topic on [Chemical Physics](#), [Energy, Fluids and Plasmas](#), [Materials Science](#) and [Mathematical Physics](#)



View Online



Export Citation



CrossMark

ARTICLES YOU MAY BE INTERESTED IN

[Zn-induced layer exchange of p- and n-type nanocrystalline SiGe layers for flexible thermoelectrics](#)

Applied Physics Letters **116**, 182105 (2020); <https://doi.org/10.1063/5.0006958>

[High photoresponsivity in a GaAs film synthesized on glass using a pseudo-single-crystal Ge seed layer](#)

Applied Physics Letters **114**, 142103 (2019); <https://doi.org/10.1063/1.5091714>

[Polycrystalline thin-film transistors fabricated on high-mobility solid-phase-crystallized Ge on glass](#)

Applied Physics Letters **114**, 212107 (2019); <https://doi.org/10.1063/1.5093952>



NEW: TOPIC ALERTS

Explore the latest discoveries in your field of research

SIGN UP TODAY!

Improving photoresponsivity in GaAs film grown on Al-induced-crystallized Ge on an insulator

Cite as: AIP Advances 10, 015153 (2020); doi: 10.1063/1.5138677

Submitted: 15 November 2019 • Accepted: 8 January 2020 •

Published Online: 28 January 2020



T. Nishida, T. Suemasu,  and K. Toko^{a)}

AFFILIATIONS

Institute of Applied Physics, University of Tsukuba, 1-1-1 Tennodai, Tsukuba, Ibaraki 305-8573, Japan

^{a)} Author to whom correspondence should be addressed: toko@bk.tsukuba.ac.jp

ABSTRACT

The highest recorded photoresponsivity in polycrystalline GaAs films on glass has been updated by precisely controlling the growth temperature of GaAs on a Ge seed layer formed by Al-induced layer exchange. X-ray diffraction and electron backscatter diffraction analyses showed that large-grained ($>100\ \mu\text{m}$) GaAs (111) films epitaxially grew from the Ge layer above $510\ ^\circ\text{C}$. According to energy dispersive x-ray and Raman spectra, $550\ ^\circ\text{C}$ was the optimum growth temperature that allowed for the growth of high-quality GaAs film with a stoichiometric composition. Reflecting the high crystallinity, the internal quantum efficiency reached 90% under a bias voltage of 0.3 V. Low-temperature GaAs films grown on inexpensive substrates will make the development of advanced solar cells that achieve both high efficiency and low cost possible.

© 2020 Author(s). All article content, except where otherwise noted, is licensed under a Creative Commons Attribution (CC BY) license (<http://creativecommons.org/licenses/by/4.0/>). <https://doi.org/10.1063/1.5138677>

The direct synthesis of polycrystalline GaAs films on inexpensive substrates has been studied for decades as a means of developing solar cells that simultaneously achieve high efficiency and low cost.^{1,2} Simple techniques, including vacuum deposition,^{3–9} crystallization of amorphous films,^{10–12} and chemical synthesis,^{13,14} have allowed for polycrystalline GaAs films on insulators; however, a photoreponse has never been obtained mainly owing to carrier recombination at grain boundaries, which often exists in the films.^{15,16}

A single-crystal Ge (c-Ge) substrate has been used as an epitaxial template for a high-quality GaAs film because its lattice matched that of GaAs.^{17–20} In line with this, research on forming large-grained Ge thin films on insulating substrates and epitaxially grown GaAs films has been widely conducted.^{21,22} Recently, conversion efficiencies exceeding 10% have been obtained with GaAs films on Ge thin films.²³ However, because the process temperature is high, the substrate is limited to a heat-resistant material such as metal.

Previously, we formed a Ge thin film on a glass substrate using Al-induced layer exchange (ALILE)^{24,25} and epitaxially grew a GaAs film on ALILE-Ge at a low temperature ($520\ ^\circ\text{C}$).²⁶ The grain size of the obtained GaAs film was so large ($>100\ \mu\text{m}$) that it could be called a pseudo-single-crystal. Reflecting the large grain size, the photoresponsivity was comparable to that of the GaAs film

formed on a single-crystal Ge substrate. In this study, we investigate the effects of GaAs growth temperature on the quality of polycrystalline GaAs films seeded by ALILE-Ge. The precise control of the growth temperature improves the crystal and optical properties of the GaAs film, resulting in the highest photoresponsivity in any GaAs film directly synthesized on a glass substrate at low temperature.

As shown in Fig. 1, we grew GaAs on ALILE-Ge to form a pseudo-single-crystal GaAs film. First, the ALILE process is as follows: an Al layer (thickness: 50 nm) was prepared and then exposed to air for 3 min to form a native AlO_x membrane, followed by preparing an amorphous Ge layer (thickness: 70 nm). The depositions were carried out using DC magnetron sputtering (base pressure: 5×10^{-5} Pa) with an Ar pressure of 6×10^{-2} Pa and a DC power of 300 W. The sample was annealed at $350\ ^\circ\text{C}$ for 50 h in N_2 , which crystallized the Ge via exchange between the Ge and Al layers. The Al layer and the Ge islands, remaining in the top layer, were removed using HF (1.5%) and H_2O_2 (50%) solutions.²⁷ Then, a GaAs layer (thickness: 500 nm) was formed by molecular beam epitaxy (MBE, base pressure: 5×10^{-8} Pa) where Ga and As atoms were supplied by Knudsen cells with a GaAs deposition rate of 200 nm/h. The GaAs layers were prepared at a growth temperature T_g ranging from 500 to $570\ ^\circ\text{C}$. For photoresponse measurement, ITO electrodes

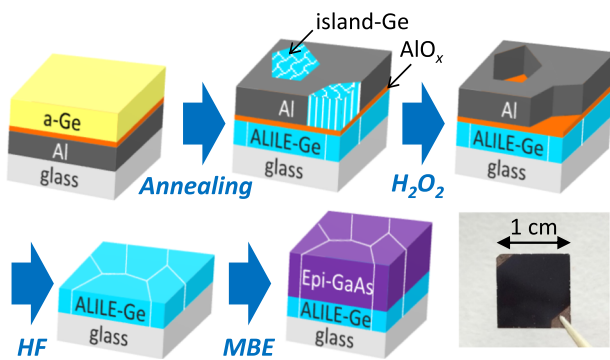


FIG. 1. Schematic of the sample preparation procedure and a photograph of the resulting sample.

(thickness: 300 nm, diameter: 1 mm) were prepared on the GaAs surface using RF magnetron sputtering at room temperature. The sample properties were evaluated by x-ray diffraction (XRD, spot diameter: 5 mm), electron backscatter diffraction (EBSD), energy dispersive x-ray spectrometry (EDX) with an accelerating voltage of 20 kV, Raman spectroscopy (spot diameter: 1 μm , wavelength: 532 nm), and photoresponsivity measurement.

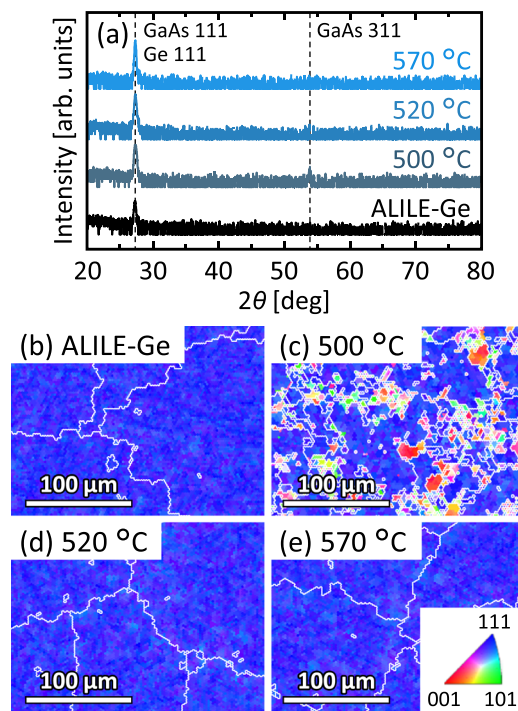


FIG. 2. Characterization of the crystal orientation of the ALILE-Ge seed layer and the representative GaAs samples for $T_g = 500^\circ\text{C}$, 520°C , and 570°C : (a) θ - 2θ XRD patterns. Out-of-plane EBSD images of the (b) ALILE-Ge and [(c)–(e)] GaAs samples where T_g is labeled in each image. The solid white lines indicate random grain boundaries; the coloration indicates the crystal orientation [refer to the legend in the inset in (e)].

As representatively shown in Fig. 2(a), all samples for $T_g = 500$ – 570°C exhibited a strong GaAs (111) peak at $\sim 27^\circ$. The ALILE-Ge seed layer also exhibited a small Ge (111) peak at $\sim 27^\circ$. The increase in the (111) peak intensity after GaAs deposition suggests the epitaxial growth of GaAs (500 nm thick) on the (111)-oriented Ge seed layer (50 nm thick). The intensity of the GaAs (111) peak slightly increases with increasing T_g , while samples at $T_g = 500^\circ\text{C}$ have a peak at $\sim 54^\circ$, corresponding to the GaAs (311) plane. Figure 2(b) shows that the ALILE-Ge seed layer is highly (111)-oriented and large-grained ($>100\ \mu\text{m}$). Figure 2(c) shows that the sample at $T_g = 500^\circ\text{C}$ has a lower (111) orientation and smaller grain size than ALILE-Ge, indicating incomplete epitaxial growth. In contrast, as representatively shown in Figs. 2(d) and 2(e), the EBSD images for the samples at $T_g \geq 510^\circ\text{C}$ were very similar to those of ALILE-Ge. The results in the XRD and EBSD analyses are consistent and indicate that the current T_g range (500 – 570°C) is very sensitive to GaAs epitaxial growth under current growth conditions.

Figure 3(a) shows that the sample at $T_g = 550^\circ\text{C}$ exhibits clear Ga and As peaks in the EDX spectra. A Si peak is also observed because of the SiO_2 glass substrate. Ge is below the detection limit of the EDX system because the Ge layer is thin and is located under GaAs. Similar EDX spectra were obtained for all samples. As representatively shown in Fig. 3(b), all samples exhibited sharp peaks in the Raman spectra, corresponding to the transverse optical (TO) mode ($\sim 270\ \text{cm}^{-1}$) and the longitudinal optical (LO) mode ($\sim 290\ \text{cm}^{-1}$) of crystalline GaAs.^{7,10} The composition of GaAs and the FWHMs of the TO and LO mode peaks were calculated from the EDX and Raman spectra, respectively, and are summarized in

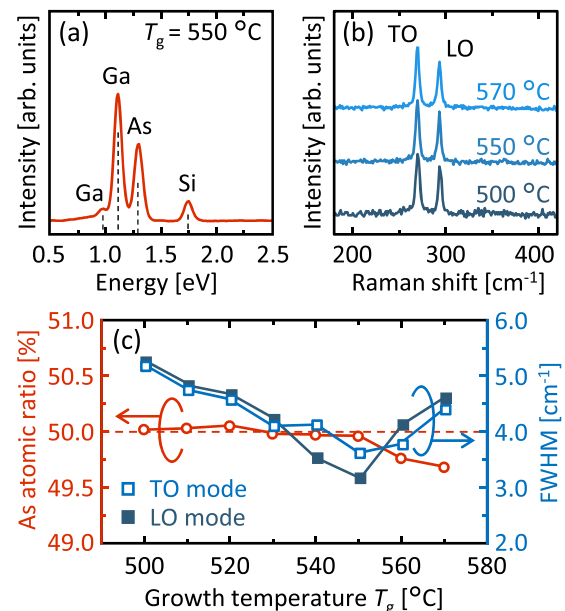


FIG. 3. Characterization of the composition and crystal quality of the samples for $T_g = 500$ – 570°C : (a) EDX spectrum of the sample at $T_g = 550^\circ\text{C}$. (b) Raman spectra of the samples for $T_g = 500^\circ\text{C}$, 550°C , and 570°C , and (c) the As atomic ratio derived from EDX spectra and FWHMs of the TO and LO mode Raman peaks as a function of T_g .

Fig. 3(c). The As atomic ratio in the GaAs layer is constant at 50% for $T_g = 500\text{--}550\text{ }^\circ\text{C}$ and decreases for $T_g > 550\text{ }^\circ\text{C}$. This behavior is likely due to the evaporation of As atoms on the surface during MBE at high temperatures. Figure 3(c) also shows that the FWHMs initially decrease with increasing T_g , indicating that the higher T_g improves the crystallinity of the GaAs films. Conversely, the FWHMs increase for $T_g > 550\text{ }^\circ\text{C}$, which is likely due to the inappropriate stoichiometry of GaAs. These results indicate that the sample at $T_g = 550\text{ }^\circ\text{C}$ has the highest crystallinity of GaAs. The growth temperature is almost consistent with that of GaAs on a c-Ge(111) substrate.^{19,20}

Photoresponsivity measurement was conducted after the preparation of ITO electrodes on the GaAs surface. The resistivity of ALILE-Ge is low enough ($<10^{-3}\text{ }\Omega\text{ cm}$) to be used as a bottom electrode because of high Al doping in Ge.²⁸ To transfer the photogenerated electrons in the GaAs films to a surface ITO electrode, bias voltages of 0.3 V were applied to ITO with respect to ALILE-Ge. Figure 4(a) shows clear photoresponse spectra rising near a wavelength of 900 nm, which corresponds to the bandgap of GaAs. Figure 4(b) shows that internal quantum efficiency (IQE) is maximum at wavelengths of 700–800 nm for all samples. The photoresponsivity and IQE strongly depend on T_g . As the photoresponsivity increases, the short wavelength side (500–700 nm) exhibits a relatively smaller photoresponsivity than the long wavelength side (700–800 nm) for each spectrum. Because the short wavelength side corresponds to the absorption near the surface, this behavior suggests that the GaAs surface region has defects, including dangling bonds. Surface passivation using Al compounds, such as AlGaAs, will be effective in improving photoresponsivity.^{17,23} Figure 4(c) shows that for both ALILE-Ge and c-Ge samples, the photoresponsivity and IQE initially increase with increasing T_g and decrease for $T_g > 550\text{ }^\circ\text{C}$. This behavior is consistent with the

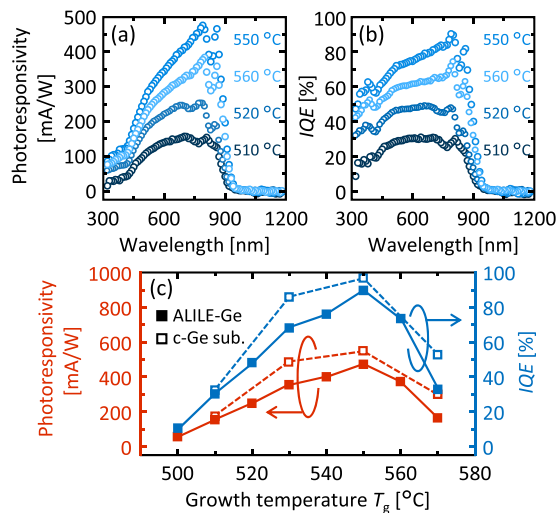


FIG. 4. Photoresponse properties of the samples for $T_g = 500\text{--}570\text{ }^\circ\text{C}$, where the bias voltage is 0.3 V: (a) photoresponsivity and (b) IQE spectra of the samples for $T_g = 510\text{ }^\circ\text{C}$, $520\text{ }^\circ\text{C}$, $550\text{ }^\circ\text{C}$, and $560\text{ }^\circ\text{C}$ and (c) maximum photoresponsivity and IQE values for each spectrum as a function of T_g , where the data for GaAs on a c-Ge(111) substrate are also shown for comparison.

FWHM results, as shown in Fig. 3(c). We note that the photoresponsivity and IQE of the ALILE-Ge samples are comparable to those of the c-Ge samples. This is because GaAs on ALILE-Ge is large-grained and behaves like a pseudosingle crystal. Thus, maximum photoresponsivity (470 mA/W) and IQE (90%) were obtained at $T_g = 550\text{ }^\circ\text{C}$.

In conclusion, we updated the highest photoresponsivity among polycrystalline GaAs films synthesized on a glass substrate. The crystal and optical properties of the GaAs films strongly depended on T_g because high T_g simultaneously provides high crystallinity and broken stoichiometric composition due to As evaporation. The maximum IQE reached 90% at $T_g = 550\text{ }^\circ\text{C}$ under a bias voltage of 0.3 V. The findings in the present study will contribute to the development of high-efficiency thin-film solar cells with III-V compound semiconductors based on low-cost substrates.

This work was supported financially by JSPS KAKENHI (Grant No. 17H04918). The authors are grateful to Dr. Y. Tominaga (Hiroshima University) for helpful discussions. Some experiments were conducted at the International Center for Young Scientists at NIMS and the Nanotechnology Platform at the University of Tsukuba.

REFERENCES

- R. Venkatasubramanian, E. Siivola, B. O'Quinn, B. Keyes, and R. Ahrenkiel, *AIP Conf. Proc.* **404**, 411 (1997).
- J. Yoon, S. Jo, I. S. Chun, I. Jung, H.-S. Kim, M. Meitl, E. Menard, X. Li, J. J. Coleman, U. Paik, and J. A. Rogers, *Nature* **465**, 329 (2010).
- J. J. Yang, P. D. Dapkus, R. D. Dupuis, and R. D. Yingling, *J. Appl. Phys.* **51**, 3794 (1980).
- S. Tsuji, E. Iri, and H. Takakura, *Jpn. J. Appl. Phys.* **31**, 880 (1992).
- K. Mochizuki, T. Nakamura, T. Mishima, H. Masuda, and T. Tanoue, *J. Electron. Mater.* **23**, 577 (1994).
- M. Imaizumi, M. Adachi, Y. Fujii, Y. Hayashi, T. Soga, T. Jimbo, and M. Umeno, *J. Cryst. Growth* **221**, 688 (2000).
- A. Erlacher, B. Ullrich, E. Y. Komarova, H. Jaeger, H. J. Haugan, and G. J. Brown, *J. Non-Cryst. Solids* **352**, 193 (2006).
- Y. Kajikawa, T. Okuzako, S. Takami, and M. Takushima, *Thin Solid Films* **519**, 136 (2010).
- V. Şenay, S. Özen, S. Pat, and Ş. Korkmaz, *J. Alloys Compd.* **663**, 829 (2016).
- R. Campomanes, J. Dias da Silva, J. Vilcarromero, and L. Cardoso, *J. Non-Cryst. Solids* **299-302**, 788 (2002).
- J. H. Epple, K. L. Chang, C. F. Xu, G. W. Pickrell, K. Y. Cheng, and K. C. Hsieh, *J. Appl. Phys.* **93**, 5331 (2003).
- D. Pirzada and G. J. Cheng, *J. Appl. Phys.* **105**, 093114 (2009).
- J. Nayak and S. N. Sahu, *Appl. Surf. Sci.* **182**, 407 (2001).
- S. Sathasivam, R. R. Arnepalli, B. Kumar, K. K. Singh, R. J. Visser, C. S. Blackman, and C. J. Carmalt, *Chem. Mater.* **26**, 4419 (2014).
- M. Yamaguchi and Y. Itoh, *J. Appl. Phys.* **60**, 413 (1986).
- S. R. Kurtz and R. McConnell, *AIP Conf. Proc.* **404**, 191 (1997).
- M. Yamaguchi, T. Takamoto, K. Araki, and N. Ekins-Daukes, *Sol. Energy* **79**, 78 (2005).
- R. R. King, D. C. Law, K. M. Edmondson, C. M. Fetzer, G. S. Kinsey, H. Yoon, R. A. Sherif, and N. H. Karam, *Appl. Phys. Lett.* **90**, 183516 (2007).
- Y. Kajikawa, Y. Son, H. Hayase, H. Ichiba, R. Mori, K. Ushirogouchi, and M. Irie, *J. Cryst. Growth* **477**, 40 (2017).
- D. Pelati, G. Patriarche, O. Mauguin, L. Largeau, L. Travers, F. Brisset, F. Glas, and F. Oehler, *J. Cryst. Growth* **519**, 84 (2019).
- M. G. Mauk, J. R. Balliet, and B. W. Feyock, *J. Cryst. Growth* **250**, 50 (2003).

- ²²C.-Y. Tsao, J. Huang, X. Hao, P. Campbell, and M. A. Green, *Sol. Energy Mater. Sol. Cells* **95**, 981 (2011).
- ²³P. Dutta, M. Rathi, D. Khatiwada, S. Sun, Y. Yao, B. Yu, S. Reed, M. Kacharia, J. Martinez, A. P. Litvinchuk, Z. Pasala, S. Pouladi, B. Eslami, J.-H. Ryou, H. Ghasemi, P. Ahrenkiel, S. Hubbard, and V. Selvamianickam, *Energy Environ. Sci.* **12**, 756 (2019).
- ²⁴K. Toko, M. Kurosawa, N. Saitoh, N. Yoshizawa, N. Usami, M. Miyao, and T. Suemasu, *Appl. Phys. Lett.* **101**, 072106 (2012).
- ²⁵K. Toko, R. Numata, N. Oya, N. Fukata, N. Usami, and T. Suemasu, *Appl. Phys. Lett.* **104**, 022106 (2014).
- ²⁶T. Nishida, K. Moto, N. Saitoh, N. Yoshizawa, T. Suemasu, and K. Toko, *Appl. Phys. Lett.* **114**, 142103 (2019).
- ²⁷K. Toko, K. Nakazawa, N. Saitoh, N. Yoshizawa, and T. Suemasu, *Cryst. Growth Des.* **15**, 1535 (2015).
- ²⁸K. Kusano, A. Yamamoto, M. Nakata, T. Suemasu, and K. Toko, *ACS Appl. Energy Mater.* **1**, 5280 (2018).